IEEE Access
Multidisciplinary | Rapid Review | Open Access Journal

Received February 13, 2017, accepted March 7, 2017, date of publication April 5, 2017, date of current version May 17, 2017.

Digital Object Identifier 10.1109/ACCESS.2017.2690990

Modeling and Performance Analysis of Metallic Plasmonic Nano-Antennas for Wireless Optical Communication in Nanonetworks

MONA NAFARI, (Student Member, IEEE), AND JOSEP MIQUEL JORNET, (Member, IEEE)
Department of Electrical Engineering, University at Buffalo, The State University of New York, Buffalo, NY 14260, USA

Corresponding author: M. Nafari (monanafa@buffalo.edu)

This work was supported by the U.S. National Science Foundation under Grant CBET-1445934 and Grant CBET-1555720.

ABSTRACT In this paper, metallic plasmonic nano-antennas are modeled and analyzed for wireless optical communication. More specifically, a unified mathematical framework is developed to investigate the performance in transmission and reception of metallic nano-dipole antennas. This framework takes into account the metal properties, i.e., its dynamic complex conductivity and permittivity; the propagation properties of surface plasmon polariton waves on the nano-antenna, i.e., their confinement factor and propagation length; and the antenna geometry, i.e., length and radius. The generated plasmonic current in reception and the total radiated power and efficiency in transmission are analytically derived by utilizing the framework. In addition to numerical results, the analytical models are validated by means of simulations with COMSOL Multi-physics. The developed framework will guide the design and development of novel nano-antennas suited for wireless optical communication.

INDEX TERMS Wireless optical communication, nanophotonics, plasmonics, nano-antenna, nanonetworks.

I. INTRODUCTION

Nanotechnology is providing the engineering community with a new set of tools to design and manufacture novel nanoscale devices, which are able to perform simple tasks, such as computing, data storing, sensing and actuation. The integration of several of these nano-devices into a single entity will enable the development of advanced nanoscale machines. By means of communication, nanomachines will be able to organize themselves in networks, or nanonetworks, and complete more complex tasks in a distributed fashion, such as wireless nanosensor networks for chemical and biological attack prevention [2], advanced health monitoring systems [3], agricultural and plant monitoring [4], optimization and control of chemical reactors [5], or wireless networks on chip [6].

From the electromagnetic (EM) perspective, the miniaturization of a conventional metallic antenna to meet the size requirements of a nanomachine would theoretically result in very high resonance frequencies. For example, according to classical antenna theory, a one-micrometer-long metallic antenna would radiate at approximately 150 THz. This is only true if the material of the antenna building components is assumed to be a perfect electrical conductor (PEC), i.e., a material with infinite conductivity. However, at the aforementioned frequencies, metals no longer behave as PEC [7]. On the contrary, the conductivity of metals such as gold or silver [8]; metamaterials, i.e., engineered materials with rationally designed arrangements of nano-structured building blocks [9]; as well as nanomaterials such as graphene [10], is a frequency-dependent complex-valued magnitude.

The material conductivity affects the way in which a current wave propagates in the nano-antenna. In particular, the global oscillations of electrical charge in close proximity to the surface of the antenna building components, i.e., within the so called penetration depth, results into the excitation of a confined EM wave at the surface of the antenna. This peculiar EM wave is commonly referred to as a surface plasmon polariton (SPP) wave. The frequency at which SPP waves are excited depends on the material conductivity of the antenna building components. For example, graphene supports SPP waves at frequencies as low as in the THz band (0.1-10 THz) [11], whereas in noble metals such as gold or silver, SPP waves are only observed at tens of THz and above [7].

Starting from this result, the field of plasmonic nano-antennas in the THz band and above has been gaining

momentum. In [12], we proposed for the first time the use of graphene to develop THz plasmonic nano-antennas and, since then, many related works and extensions have followed [13]–[16]. For the time being, however, one of the main challenges at THz frequencies is posed by the lack of efficient THz sources, needed to drive the nano-antennas [17].

When it comes to infrared and visible optical frequencies, the possibility for the first time to create precise accurate nano-structures, comparable to the optical wavelengths in their largest dimensions and with very high aspect ratios, has motivated the development of optical nano-antennas [18], [19]. In this case, optical sources such as nano-lasers, [20], [21], are more readily available. As explained in Sec. II, many works on the design of optical nano-antennas can be found in the literature. However, to the best of our knowledge, a unified mathematical framework able to relatee material properties, SPP wave behavior and the nano-antenna geometry with communication-relevant parameters, such as gain in transmission and reception is missing.

In this paper, we model and analyze the performance of metallic plasmonic nano-antennas for wireless optical communication. More specifically, we first develop a unified mathematical framework to investigate the performance in transmission and reception of nano-dipole antennas based on different metals. This framework takes into account the metal properties, i.e., its dynamic complex conductivity and permittivity; the propagation properties of SPP waves on the nano-antenna, i.e., their confinement factor and propagation length; and the antenna geometry, i.e., length and radius. By utilizing the framework, the generated plasmonic current in reception and the total radiated power and efficiency in transmission are analytically derived. To validate the model, we conduct extensive simulations with COMSOL Multi-physics. Finally, by utilizing the model, we numerically investigate and compare the performance of the developed nano-antennas at optical frequencies and provide directions for the design of wireless optical communication systems in nanonetworks.

The remaining of this paper is organized as follows. In Sec. II, we summarize the related works on optical nano-antenna. In Sec. III, we review the fundamental working principle of a plasmonic nano-antenna, describe the conductivity model utilized in our analysis and analyze the SPP wave propagation properties. Then, in Sec. IV, we formulate the EM fields on and inside the antenna, and obtain a semi-closed form expression for the plasmonic current in the nano-antenna. We then define the antenna performance metrics in far field in section V. Numerical and simulation results are presented in Sec. VI and the paper is concluded in Sec. VII.

II. RELATED WORKS

Within the last decade, there have been several fundamental works on the development of optical nano-antennas. Cao and Jahns [22] analyzed the propagation properties of SPP waves cylindrical or rod-type nano-antennas, by formulating and solving the SPP wave dispersion equation at the radial boundary condition along the nano-antenna. They mainly illustrated that different radius exhibit different wavelength-dependent effective mode index for a cylindrical nanowire waveguide. Importantly, their findings indicate the increasing importance of skin effect for SPPs in the terahertz range and above, as well as the enhancement of such effects on curved surfaces. Moreover, in [23], the derivation of angle-dependent reflection amplitude and phase of a SPP wave at a boundary between antenna and surrounding area is presented and, in [24], the impact of the nano-antenna caps is incorporated. All these works illustrate the fact that the nano-antenna geometry heavily impacts the propagation characteristics of the SPP waves. In [25], the nano-antenna fields are characterized, starting from the estimated propagation constant of SPP waves on nanowires obtained by means of experimental measurements. Some related aspects, such as the choice of metal and the slowly decaying modal field, are also discussed in [7] and [26]. Optical properties of metals in terms of intra and interband processes as well as plasma effects are described in these materials, such that specifically [7] provides an overview of alternative plasmonic materials along with motivation for each material choice and important aspects of fabrication.

Another issue usually discussed in the related works is the need to account or not for quantum mechanical effects. If the feature size of the nano-antenna D, i.e., the smallest of the critical dimensions, is less than one nanometer, the quantum effects need to be taken into account. In this situation, solving Maxwell equations using non-local bulk dielectric functions may extend the validity of the classical treatment. For plasmonic systems with narrow junctions, quantum-mechanical electron tunneling is the major nonlocal effect that determines the optical response of the system. In the non-contact regime, for distances $D > 0.5$ nm, no significant electron transfer can occur in-between the gap; thus, this situation can be correctly described within the classical electrodynamical treatment since tunneling happens in distances of $0.1 < D < 0.5$ nm [27]. In the latter case, appropriate approaches from quantum mechanics, which usually involve the combination of Schrödinger equation with Maxwell equations, should be solved by consistently using numerical methods. In this paper, the feature size is the nano-antenna gap, which is still several nanometers long. As a result, we consider that the quantum current density, which can be used as an current additional source for the Maxwell equations, can be ignored.

III. PLASMONIC NANO-ANTENNA MODEL

A. WORKING PRINCIPLE

The plasmonic nano-antenna design considered in the analysis, is shown in Fig. 1. The nano-antenna consists of two identical metallic arms with a feeding/receiving gap in between which its size is optimized. The working principle of the nano-antenna is as follows. We explain first its functioning in reception:

- Consider an incident plane wave with polarization parallel to the plane defined by the nano-antenna long axis and the direction of the wave propagation. Following the

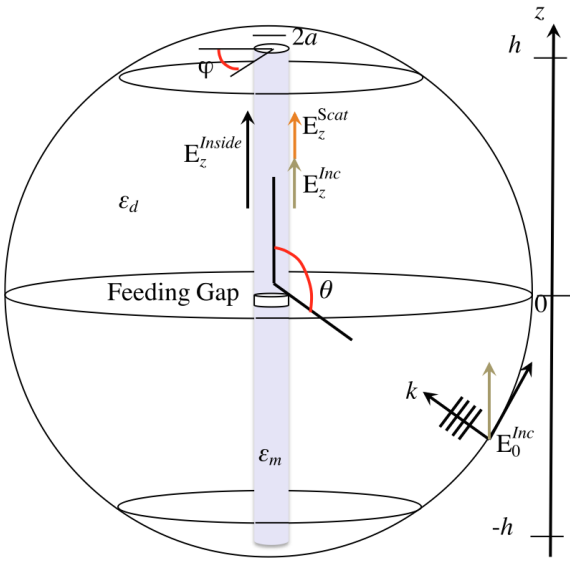

FIGURE 1. Plasmonic nano-dipole antenna considered in the analysis.

notation in Fig. 1, we are interested in the incident electric field component parallel to the z-axis, E_z^{Inc}, which is given by:

$$E_z^{\text{Inc}}(r,z) = E_0^{\text{Inc}}(r)\sin\theta e^{j(k_0\cos\theta)z} = E_{||}^{\text{Inc}}(r)\, e^{jk_{||}z}, \tag{1}$$

where E_0^{Inc} stands for the field strength, k_0 refers to the wave vector, and θ is the angle of incidence. When E_z^{Inc} irradiates the nano-antenna, it excites the free electrons within the antenna penetration depth. The electronic response of the nano-antenna to an EM field is determined by the conductivity of its building material. In Sec. III-B, we describe the conductivity model for metals that we utilize in our analysis.

- At the interface between the nano-antenna metallic arms and the surrounding medium, longitudinal SPP waves that propagate along the z-axis are excited. The SPP wave vector, k_{spp} is determined by the antenna geometry, namely, the antenna arm radius and length, as well as on the real and imaginary part of the material conductivity. In Sec. III-C, we deduce the dispersion equation for SPP waves on the antenna and analyze their propagation properties as functions of the material conductivity and antenna geometry.
- To enhance the detection of the incident EM wave, we are interested in designing a plasmonic resonant cavity. In particular, we are interested in having a resonant cavity for the fundamental resonant frequency, which depends on the SPP wave propagation speed. In Sec. IV, we analyze the nano-antenna in reception, by starting from the formulation of the electric field incident to the antenna, the electric field scattered by the antenna and the SPP wave propagating inside the antenna.

The same behavior holds in transmission due to the antenna reciprocity principle [28]. In particular, a SPP wave on the nano-antenna can be electrically excited by the feeding gap. The time-changing SPP wave, on its turn, induces a time-changing magnetic field, which on its turn generates an electric field, and this results in the propagation of an EM wave. As before, the performance of the nano-antenna in transmission depends on the conductivity of the material as well as on the geometry of the nano-antenna, which determine the SPP properties. In Sec. V, we analyze the nano-antenna performance in transmission in terms of radiated fields and resulting directivity.

TABLE 1. Parameters for the optical conductivity of metals.

Metal	ω_p [10^{15} rad/s]	τ_D [10^{-14} s]	n_e [10^{28}/m^3]
Cu	14.11	0.7685	8.47
Al	22.75	26	18.1
Ag	13.35	0.8	5.86
Au	13.8	3.3	5.9

B. OPTICAL CONDUCTIVITY MODEL FOR METALS

The conductivity of metals at optical frequencies is a complex-valued quantity. The real part of the conductivity is responsible for ohmic losses whereas the imaginary part accounts for the phase offset between the local electric field and current density [29]. There are many analytical models for the conductivity of metals. In this paper, we utilize the well-established Drude model, which takes into account the intra-band electron transitions within the metal energy band-structure [30]. Accordingly, the metal complex conductivity σ and its complex permittivity ε_m can be written as functions of the angular frequency, $\omega = 2\pi f$, as follows:

$$\begin{aligned}\sigma(\omega) &= -j(\varepsilon_m(\omega) - \varepsilon_\infty)\varepsilon_0\omega \\ &= -j\omega\varepsilon_0\left[-\frac{\omega_p^2\tau_D^2}{1+\omega^2\tau_D^2} + j\frac{\omega_p^2\tau_D}{\omega\left(1+\omega^2\tau_D^2\right)}\right],\end{aligned} \tag{2}$$

where ε_0 is the vacuum permittivity, ε_∞ is 1 for metals [31], τ_D is the electron relaxation time and ω_p stands for the plasma wave frequency, which is given by

$$\omega_p = \sqrt{\frac{n_e e^2}{m^*\varepsilon_0}}, \tag{3}$$

where n_e is the number of electrons per unit of volume, e stands for the electron charge, and m^* is the electron effective mass of the electron. In Table 1, the values for these parameters are summarized for different metals, including copper (Cu) and aluminum (Al) [26], gold (Au) [30] and silver (Ag) [32]. The choice of the best plasmonic material for a given application is a subject of discussion and research.

In Fig. 2, the real and imaginary parts of the relative permittivity for all four noble metals are shown as functions of frequency. The values of this figure is validated with actual data of [33]. The absolute value of the real and imaginary parts of

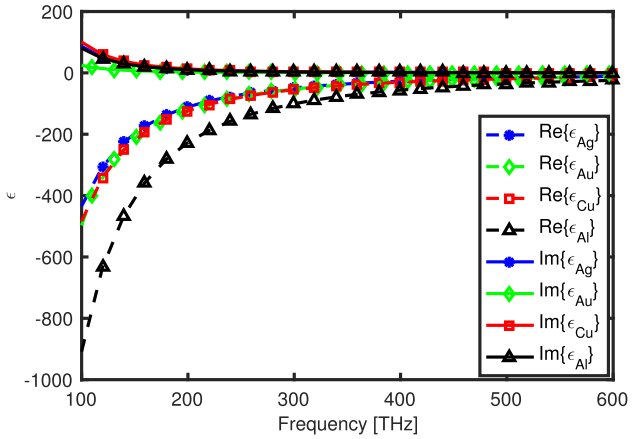

FIGURE 2. Real and imaginary parts of the relative permittivity for different nobel metals as functions of frequency.

the permittivity at higher frequencies tends to decrease, which considerably affects propagation of SPP waves, as we show in the next section.

C. SURFACE PLASMON POLARITON WAVE DISPERSION EQUATION

Next, we analytically study the propagation properties of SPP waves in the nano-antenna, by taking into account both its geometry and the complex conductivity of its building material. More specifically, we are interested in characterizing the complex SPP wave vector, k_{spp}. The real part of the wave vector, $\mathrm{Re}\{k_{spp}\}$, determines the SPP wavelength,

$$\lambda_{spp} = \frac{2\pi}{\mathrm{Re}\{k_{spp}\}}, \tag{4}$$

as well as the confinement factor k_{spp}/k_0, where $k_0 = \omega/c$ refers to free-space wave vector and c is the speed of light. The imaginary part, $\mathrm{Im}\{k_{spp}\}$, determines the SPP decay or, inversely, the SPP propagation length,

$$L = \frac{1}{2\mathrm{Im}\{k_{spp}\}}, \tag{5}$$

which is defined as the distance at which the SPP field strength has decreased by a value of $1/e$.

As mentioned before, when the antenna is illuminated by an incident plane wave, axially symmetrical SPP modes are excited. In particular, for the design of an efficient antenna, we are interested in the propagation properties of Transverse Magnetic (TM) SPP wave modes [28]. To obtain k_{spp}, we need to solve the dispersion equation for SPP waves on the nano-antenna arms. We assume that the electric field $\vec{E}$ and magnetic field $\vec{H}$ on the antenna have the following form [22]:

$$E_r(r,z) = E_r(r)\, e^{jk_{spp}z}, \tag{6}$$
$$E_z(r,z) = E_z(r)\, e^{jk_{spp}z}, \tag{7}$$
$$H_\phi(r,z) = H_\phi(r)\, e^{jk_{spp}z}. \tag{8}$$

Starting from the Maxwell's equations in their differential form and taking into account that for an axially symmetrical mode $\frac{\partial E}{\partial \phi} = 0$ and $\frac{\partial H}{\partial \phi} = 0$, the following equations can be written:

$$E_r(r,z) = \frac{-j}{\varepsilon k_0}\frac{\partial H_\phi(r,z)}{\partial z}, \tag{9}$$
$$E_z(r,z) = \frac{j}{\varepsilon k_0}\frac{1}{r}\frac{\partial\left(rH_\phi(r,z)\right)}{\partial r}, \tag{10}$$
$$H_\phi(r,z) = \frac{-j}{\mu_0 k_0}\left(\frac{\partial E_r(r,z)}{\partial z} - \frac{\partial E_z(r,z)}{\partial r}\right), \tag{11}$$

where $\varepsilon = \varepsilon_m$ is the relative permittivity of the region $z < h$ or $r < a$ and $\varepsilon = \varepsilon_d$ is the relative permittivity of the region defined by $z > h$ and $r > a$. By taking the z derivative of (8), the radial component of the electric field can be written as:

$$E_r(r,z) = \varepsilon^{-1}\frac{k_{spp}}{k_0}H_\phi(r,z). \tag{12}$$

By substituting (12) into (11) and taking again the z derivative of (8), the magnetic field can be written as:

$$H_\phi(r,z) = \frac{-jk_0\varepsilon}{k_{spp}^2 - k_0^2\varepsilon}\frac{dE_z(r,z)}{dr}. \tag{13}$$

Finally, by substituting (13) into (10), the following equation for E_z is obtained:

$$\zeta^2\frac{d^2E_z(r,z)}{d\zeta^2} + \zeta\frac{dE_z(r,z)}{d\zeta} - \zeta^2 E_z(r,z) = 0, \tag{14}$$

where $\zeta = p_{m,d}r$ and $p_{m,d} = \sqrt{k_{spp}^2 - k_0^2\varepsilon_{m,d}\mu_0}$ [22]. The solution of (14) for $E_z(r,z)$ has the form of $I_0(p_m a)$ in the metal and $K_0(p_d a)$ in the surrounding dielectric, where $I_n(.)$ and $K_n(.)$ are the generalized Bessel functions of first and second kind of order n. Substituting them into (13), and using the relations $\frac{dI_0(p_m r)}{dr} = p_m I_1(p_m r)$ and $\frac{dK_0(p_d r)}{dr} = -p_d K_1(p_d r)$, the solution of $H_\phi(r,z)$ can be determined. In particular, by taking into account the need for continuity in $E_z(r,z)$ and $H_\phi(r,z)$ at the surface of the antenna, i.e., at the interface between the surrounding dielectric and the metal, $r = a$, the following dispersion equation is obtained:

$$\frac{K_0(p_d a)\, I_1(p_m a)}{K_1(p_d a)\, I_0(p_m a)} = -\frac{\varepsilon_d p_m}{\varepsilon_m p_d}, \tag{15}$$

which can only numerically be solved. Ultimately, k_{spp} depends on the angular frequency ω, the cylinder radius a and the relative permittivities $\varepsilon_{m,d}$ of the metal and the surrounding dielectric. In Fig. 3, the confinement factor for different metal is shown as a function of frequency; which illustrates how different permittivities affects the propagation properties in metals. In Fig. 4(a), the confinement factor (4) for gold-based nano-antennas is shown as a function of frequency and for different nanowire radius. As can be seen, the confinement factor increases as the frequency increases. Also, by increasing the radius, the confinement factor will decrease. Similarly, in Fig. 4(b), the SPP wave propagation length (5) is shown as a function of the frequency; the smaller the radius, the shorter the SPP propagation length becomes.

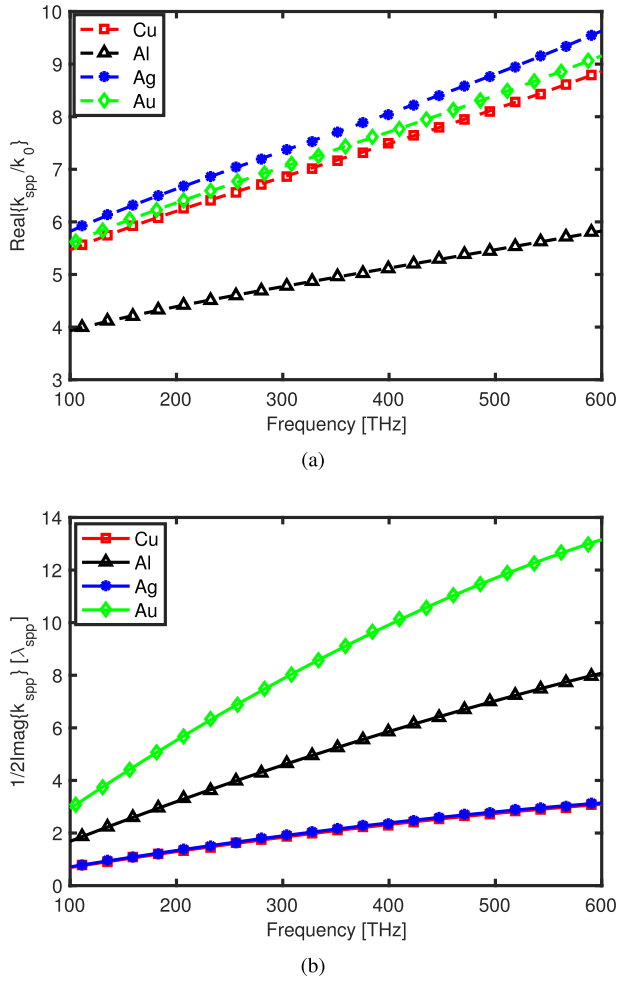

FIGURE 3. Propagation properties of SPP TM modes for different metal nanowires, radius $a = 5$ nm. (a) Confinement factor. (b) Propagation length.

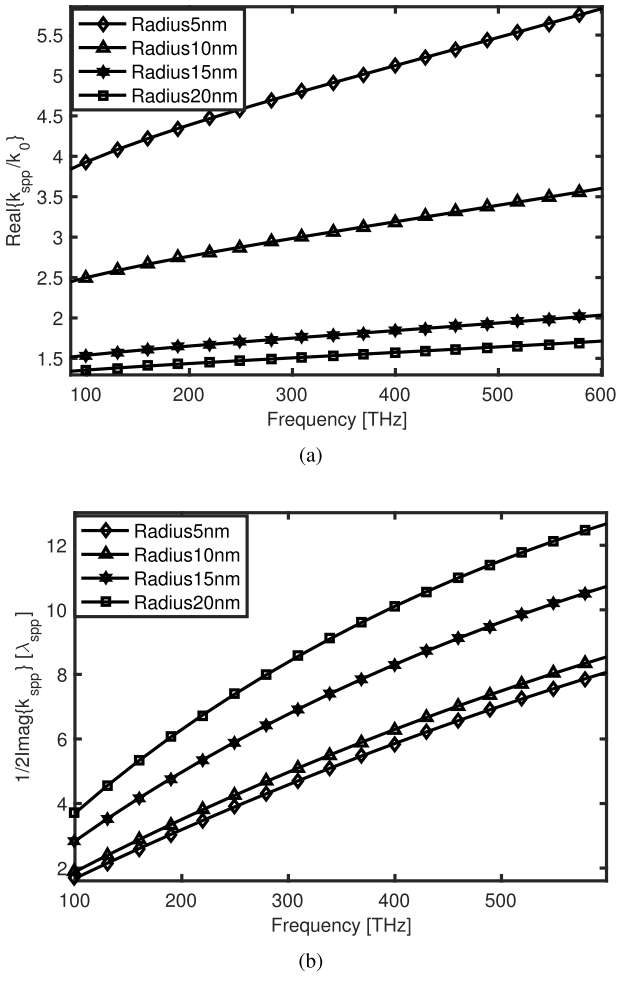

FIGURE 4. Propagation properties of SPP TM modes on gold nanowires, for different radius. (a) Confinement factor. (b) Propagation length.

D. EFFECTIVE RESONANCE LENGTH

Besides the boundary condition imposed in the radial direction, there is another boundary effect that alters the propagation of SPP waves on the nano-antenna: the caps at the two ends. SPP waves travel along the wire length l with a propagation constant k_{spp} and suffer a reflection at the two caps. To incorporate such effect in the analysis, the reflection coefficient $\mathcal{R}$ at the cap needs to be computed.

Following the methodology introduced in [24], by taking into account the boundary condition at the cap, we can write:

$$E_r\left(r, z = h^-\right) = (1 + \mathcal{R})\,\frac{\mathrm{Re}\{k_{spp}\}}{\omega\varepsilon_0\varepsilon}F(r), \tag{16}$$

$$H_\phi\left(r, z = h^-\right) = (1 - \mathcal{R})\,F\left(r\right), \tag{17}$$

with

$$F\left(r\right) = \begin{cases} \dfrac{I_1(p_m r)}{I_1(p_m a)},\ \varepsilon = \varepsilon_m & \text{if } r < a, \\ \dfrac{K_1(p_d r)}{K_1(p_d a)},\ \varepsilon = \varepsilon_d & \text{if} r > a, \end{cases} \tag{18}$$

and

$$E_r\left(r, z = h^+\right) = \int_0^{+\infty} t\left(\eta\right)\frac{\sqrt{k_0^2\varepsilon_d - \eta^2}}{\omega\varepsilon_d\varepsilon_0}J_1\left(\eta\mathcal{R}\right)\,d\eta, \tag{19}$$

$$H_\phi\left(r, z = h^+\right) = \int_0^{+\infty} t\left(\eta\right)J_1\left(\eta\mathcal{R}\right)\,d\eta, \tag{20}$$

where $J_1\left(.\right)$ is the first order Bessel function of the first kind. To solve the reflection coefficient $\mathcal{R}$, first we should find t.

Hence by using the orthogonality property of Bessel functions of the first kind, (19) is equated to (16), both sides multiplied by $J_1(\eta r)r$ and then integrated from 0 to ∞ over r to have:

$$t(\eta) = (1 + \mathcal{R})\,\frac{\eta a\varepsilon_d\mathrm{Re}\{k_{spp}\}}{\varepsilon_0\omega\sqrt{k_0^2\varepsilon_d - \eta^2}}[A_1\left(\eta\right) + A_2\left(\eta\right)], \tag{21}$$

where

$$A_1\left(\eta\right) = \frac{p_m I_2\left(p_m a\right)J_1\left(\eta a\right) + \eta I_1(p_m a)J_2\left(\eta a\right)}{I_1(p_m a)\varepsilon_m(\eta^2 + p_m^2)} \tag{22}$$

and

$$A_2(\eta) = \frac{p_d K_2(p_d a) J_1(\eta a) - \eta K_1(p_d a) J_2(\eta a)}{K_1(p_d a)\varepsilon_d\left(\eta^2 + p_d^2\right)}. \quad (23)$$

For the magnetic field H_ϕ, (20) is equated to (17). By multiplying both sides by $\frac{F(r)r}{\varepsilon}$, then integrating from 0 to ∞ over r, the final result would be:

$$\mathcal{R} = \frac{1-G}{1+G}, \quad (24)$$

where G is given by:

$$G = \frac{\int_0^{+\infty} \frac{2\eta\varepsilon_d \mathrm{Re}\{k_{spp}\}}{\sqrt{k_0^2\varepsilon_d - \eta^2}}[A_1(\eta) + A_2(\eta)]^2\, d\eta}{\frac{I_1(p_m a)^2 - I_0(p_m a)I_2(p_m a)}{\varepsilon_m I_1(p_m a)^2} - \frac{K_1(p_d a)^2 - K_0(p_d a)K_2(p_d a)}{\varepsilon_d K_1(p_d a)^2}}. \quad (25)$$

Finally, the resonances of the nanowire can be calculated by considering the propagation of the SPP wave along the nanowire and reflection at two caps as [24]:

$$l_{res} = \frac{n\pi - \varphi}{\mathrm{Re}\{k_{spp}\}}, \quad (26)$$

where n is the resonance order, φ is the phase of the reflection coefficient $\mathcal{R}$ calculated from (24), and k_{spp} is the wave vector calculated by (15). As before, this can only be numerically solved. In Fig. 5, the resonance length for gold-based nano-antennas is shown as a function of frequency. The length of a resonance optical nano-antenna is shorter than what an ideal PEC antenna would require to resonate at the same frequency, due to the large confinement factor of SPP waves in noble metal nanowires.

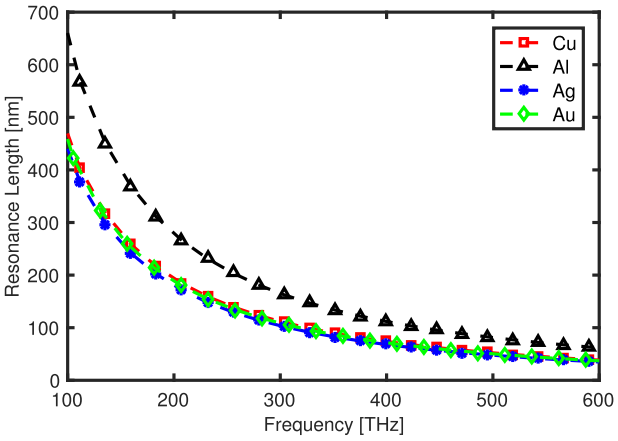

FIGURE 5. Resonance length of a plasmonic nano-antenna as a function of frequency for different metals (radius $a = 5$ nm).

IV. PLASMONIC NANO-ANTENNA PERFORMANCE IN RECEPTION

In reception, we are interested in characterizing the plasmonic current generated at the nano-antenna as a result of the incident EM wave. In order to determine the plasmonic current, we follow the conventional vector potential approach [28], but contrary to classical antenna theory for PEC antennas, we take into account that there is an electric field inside the antenna, within the penetration depth, which is the SPP wave that propagates with k_{spp}.

At the nanowire surface, the following boundary condition between the plasmonic field inside the nano-antenna, the incident field on the nano-antenna and the scattered field by the nano-antenna needs to be satisfied:

$$E_z^{\mathrm{Inside}}(r,z) = E_z^{\mathrm{Inc}}(r,z) + E_z^{\mathrm{Scat}}(r,z). \quad (27)$$

To simplify the analysis, we make the assumption that the nanowire is effectively very thin and, thus, the current density J_z, the vector potential A_z and the electric field inside the antenna E_z^{Inside} depend only on z but not on r, i.e.,

$$J_z(r,z) \approx J_z(z), \quad (28)$$

$$A_z(r,z) \approx A_z(z), \quad (29)$$

$$E_z^{\mathrm{Inside}}(r,z) \approx E_z^{\mathrm{Inside}}(z). \quad (30)$$

The field inside the nano-antenna E_z^{Inc} in (27) is related to the current density through the material conductivity, σ given by (2), i.e.,

$$J_z(z) = \sigma(\omega) E_z^{\mathrm{Inside}}(z). \quad (31)$$

The incident field E_z^{Inc} in (27) on the nano-antenna surface is given by (1).

From [34], the scattered field by the nano-antenna, E_z^{Scat} in (27), can be written as

$$E_z^{\mathrm{Scat}}(a,z) = \frac{jc^2}{\omega}\left(\frac{\partial^2}{\partial z^2} + k_0^2\right) A_z(a,z), \quad (32)$$

where

$$A_z(z) \approx \frac{\mu_0}{4\pi}\bar{Z} J_z(z), \quad (33)$$

and $\bar{Z}$ is the characteristic impedance of the wire, given by

$$\bar{Z} = \frac{4\pi}{(\varepsilon_m - 1)(k_{spp}^2 - k_0^2)}, \quad (34)$$

where ε_m is the metal permittivity given in (2) and k_{spp} is the SPP wave vector obtained from (15).

By combining (31), (32), (33), (34), and (1) in (27), the following inhomogeneous differential equation is obtained:

$$E_{||}^{\mathrm{Inc}} e^{jk_{||}z} + \frac{jc^2}{\omega}\left(\frac{\partial^2}{\partial z^2} + k_0^2\right)\frac{\mu_0}{4\pi}\bar{Z} J_z(z) = \frac{1}{\sigma(\omega)} J_z(z). \quad (35)$$

Then, as analytically shown in [25] and [34], the total current in the nano-antenna J_z can be written as the combination of the following terms

$$J_z(z) = J_{||} e^{jk_{||}z} + J_{\pm p} e^{\pm jk_{spp}z}, \quad (36)$$

where $J_{||}e^{ik_{||}z}$ is induced by the illuminating field along the wire and $J_{\pm p}$ refers to two counter-propagating plasmonic current densities propagating with k_{spp}.

By combining (36) and (35), an expression for $J_{||}$ can be found:

$$J_{||} = \sigma(\omega)\frac{(k_{spp}^2 - k_0^2)}{k_{spp}^2 - k_{||}^2} E_{||}^{\mathrm{Inc}}. \quad (37)$$

By considering the role of the wire end caps as a hard boundary and the vanishing total current density, an expression for $J_{\pm p}$ is obtained as:

$$J_{\pm p} = -J_{||}\frac{\sin((k_{spp} \pm k_{||})h)}{\sin(2k_{spp}h)}, \tag{38}$$

where $h = \frac{l}{2}$ and l stands for the length of wire given by (26). Finally, by combining (38) and (37), the plasmonic current density can be obtained as a function of the incident field E_z^{inc}. As before, this can only be numerically done.

V. ANTENNA PROPERTIES IN TRANSMISSION

By leveraging the analysis in reception, we now extend the study to the nano-antenna in transmission and, in particular, we focus on the first resonance frequency, i.e., n=1 in (26). We follow the standard vector potential approach to compute the radiated fields, with the peculiarity of having a plasmonic excitation current. For this, we consider the nano-antenna to be excited by a sinusoidal plasmonic current distribution J_z given by

$$\begin{aligned} J_z(\mathbf{x}) &= J_0 \sin\left(k_{spp}\left(\frac{l}{2} - z\right)\right)\delta(x)\,\delta(y) \\ &= J_0 \sin\left(\frac{n\pi}{2} - k_{spp}z\right)\delta(x)\,\delta(y), \end{aligned} \tag{39}$$

where $\mathbf{x} = \{x, y, z\}$ and k_{spp} is the excitation SPP wave propagation constant. The vector potential A is then defined as

$$A_z(\mathbf{x}) = \frac{\mu_0}{4\pi}\int J(\mathbf{x}')\frac{e^{jk_0|\mathbf{x}-\mathbf{x}'|}}{|\mathbf{x}-\mathbf{x}'|}d^3\mathbf{x}', \tag{40}$$

where the integral is done over the volume of the nano-antenna. If we focus in the far field, $|\mathbf{x}| \gg |\mathbf{x}'|$, $|\mathbf{x}-\mathbf{x}'| \approx r - \mathbf{n}.\mathbf{x}'$ and $r = |\mathbf{x}|$ ($\mathbf{n}$ is the unit vector in the $\mathbf{x}$ direction), we can approximate the vector potential as

$$\lim_{k_0 r\to\infty} A_z(\mathbf{x}) = \frac{\mu_0}{4\pi}\frac{e^{jk_0 r}}{r}\int J(\mathbf{x}')\,e^{-jk_0\mathbf{n}\mathbf{x}'}d^3\mathbf{x}'. \tag{41}$$

By substituting (39) in (41), again considering only the first resonance and recalling Euler's formula $e^{jk_{spp}z'} + e^{-jk_{spp}z'} = 2\cos(k_{spp})z'$, the vector potential can be rewritten as

$$\begin{aligned} &\lim_{k_0 r\to\infty} A_z(\mathbf{x}) \\ &= J_0\frac{\mu_0}{4\pi}\frac{e^{jk_0 r}}{r}\int_{-h}^{+h}\sin\left(\frac{n\pi}{2} - k_{spp}z'\right)e^{-jz'k_{||}}dz' \\ &= J_0\frac{\mu_0}{8\pi}\frac{e^{jk_0 r}}{r}\left(\frac{e^{j(k_{spp}-k_{||})z'}}{k_{spp}-k_{||}} - \frac{e^{-j(k_{spp}+k_{||})z'}}{k_{spp}+k_{||}}\right)\Bigg|_{-h}^{+h} \end{aligned} \tag{42}$$

where $k_{||} = k_0\cos\theta$, as defined in Sec. III. By solving the vector potential integral (42) on the wire from $-\frac{\pi}{2k_{spp}}$ to $\frac{\pi}{2k_{spp}}$ for the first resonance, the magnetic field H and the electric field E are obtained as:

$$\begin{aligned} H_\phi(\mathbf{x}) &= \frac{1}{\mu_0}\nabla\times A(\mathbf{x}) \\ &\approx \frac{J_0}{4\pi}\frac{e^{jk_0 r}}{r}k_0\sin\theta\frac{2jk_{spp}\cos\left(\frac{k_{||}}{k_{spp}}\frac{\pi}{2}\right)}{k_{spp}^2 - k_{||}^2}, \end{aligned} \tag{43}$$

and

$$\begin{aligned} E_\theta(\mathbf{x}) &= \frac{j}{k_0}\sqrt{\frac{\mu_0}{\varepsilon_0}}\nabla\times H(\mathbf{x}) \\ &\approx \sqrt{\frac{\mu_0}{\varepsilon_0}}\frac{J_0}{4\pi}\frac{e^{jk_0 r}}{r}k_0\sin\theta\frac{2jk_{spp}\cos\left(\frac{k_{||}}{k_{spp}}\frac{\pi}{2}\right)}{k_{spp}^2 - k_{||}^2}. \end{aligned} \tag{44}$$

Next, the radiation intensity can be calculated as

$$\begin{aligned} U_{rad}(\theta,\phi) &= \frac{r^2}{2}\text{Re}[E\times H^*] \\ &= \sqrt{\frac{\mu_0}{\varepsilon_0}}\frac{J_0^2 k_0^2}{8\pi^2}\sin^2\theta\left(\frac{k_{spp}\cos\left(\frac{k_{||}}{k_{spp}}\frac{\pi}{2}\right)}{k_{spp}^2 - k_{||}^2}\right)^2, \end{aligned} \tag{45}$$

and now the total radiated power is found by integrating U_{rad} over the entire space:

$$\begin{aligned} P_{rad} &= \int_0^{2\pi}\int_0^{\pi} U_{rad}(\theta,\phi)\sin\theta d\theta d\phi \\ &= \sqrt{\frac{\mu_0}{\varepsilon_0}}\frac{J_0^2 k_0^2}{4\pi}\int_0^{+\pi}\sin^3\theta\left(\frac{k_{spp}\cos\left(\frac{k_{||}}{k_{spp}}\frac{\pi}{2}\right)}{k_{spp}^2 - k_{||}^2}\right)^2 d\theta, \end{aligned} \tag{46}$$

which can be numerically solved.

Another metric of interest is the radiation efficiency e_r, which is defined as the fraction of the power delivered to the radiation resistance R_r, [28], [35]:

$$e_r = \frac{R_r}{R_r + R_L}, \tag{47}$$

where the high-frequency resistance R_L is used to represent the conduction-dielectric losses associated with the antenna structure based on a uniform current distribution and is computed using (2) as:

$$R_L = \frac{l}{p_a}\sqrt{\frac{\omega\mu_0}{2\sigma(\omega)}}, \tag{48}$$

where l is length of antenna and $p_a = 2\pi a$ is the perimeter of the cross section of the antenna for a circular wire of radius a. The radiation resistance R_r in (47) represents the transfer of energy to the free-space wave from the antenna, and is obtained as:

$$\begin{aligned} R_r &= \frac{2P_{rad}}{I_0^2} \\ &= \frac{1}{2\pi}\sqrt{\frac{\mu_0}{\varepsilon_0}}\int_0^{+\pi} k_0^2\sin^3\theta\left(\frac{k_{spp}\cos\left(\frac{k_{||}}{k_{spp}}\frac{\pi}{2}\right)}{k_{spp}^2 - k_{||}^2}\right)^2 d\theta. \end{aligned} \tag{49}$$

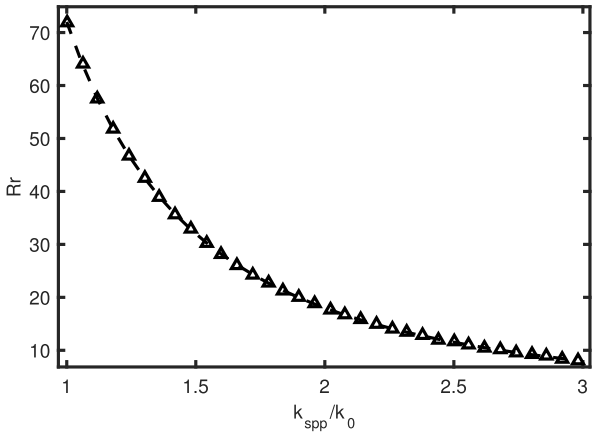

FIGURE 6. Radiation resistance of plasmonic nano-antenna as a function of $\frac{k_{spp}}{k_0}$.

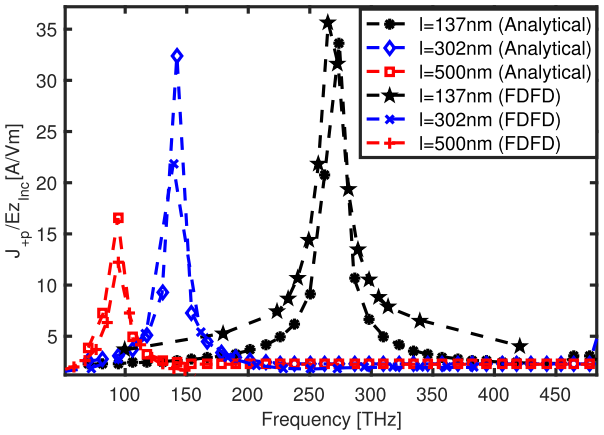

FIGURE 7. Plasmonic current on a gold-based nano-antenna as a function of frequency and length (radius $a = 5$ nm).

Note that when $\lim \frac{k_{spp}}{k_0} \rightarrow 1$ at $\theta = \frac{\pi}{2}$ or confinement factor tends to decrease, we approach the traditional radiation resistance of $\lambda/2$ dipole, i.e., 73 Ω (Fig. 6).

Both the radiated power (46) and the radiation efficiency (47) depend on k_{spp}. For the special case of a classical antenna ($k_{spp} = k_0$) (45) is reduced to:

$$U_{rad}(\theta, \phi) = \frac{J_0^2}{8\pi^2}\sqrt{\frac{\mu_0}{\varepsilon_0}}\left(\frac{\cos(\frac{\pi}{2}\cos\theta)}{\sin\theta}\right)^2, \qquad (50)$$

which is the known result for ideal PEC antennas and, similarly, (34) is simplified as well. In the next section, we numerically investigate the radiation efficiency of optical nano-antennas.

VI. NUMERICAL RESULTS

In this section, we validate the developed models by means of electromagnetic simulations with COMSOL Multi-physics (Finite Different Frequency Domain FDFD simulations) and we utilize the models to numerically investigate the performance of nano-antennas in reception and in transmission. As a reference,

A. ANTENNA PERFORMANCE IN RECEPTION

We numerically solve the plasmonic current density $J_{\pm p}$ given by (38), which depends on its turn on the SPP wave propagation constant k_{spp}, resonant length l and material conductivity σ parameters given by (15), (26) and (2), respectively. In addition, we utilize COMSOL Multi-physics to validate our results by means of FDFD simulations, in which the only required initial parameter is the material conductivity σ.

In Figure 7, the plasmonic current density is shown as a function of the illumination frequency f for three different nano-antenna lengths l, namely, 500 nm, 302 nm and 150 nm. For these results, gold-based nano-antennas with 5 nm radius are considered. Clear resonances can be observed at 91 THz, 140 THz and 270 THz, respectively. The z-component of the current density and its maximum is taken from analytically produced data and FDFD simulations for different length and

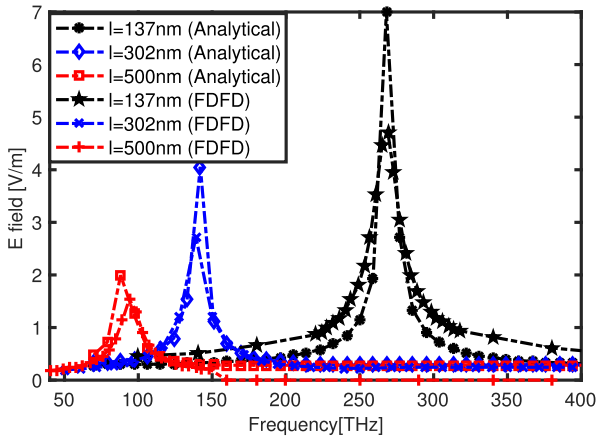

FIGURE 8. Radiated field by a gold-based nano-antenna as a function of frequency and length (radius $a = 5$ nm.

frequencies are performed for validation purposes. There is good agreement between the numerical and the simulation results. As expected, the high confinement factor of SPP waves in actual metals results into significantly smaller nano-antennas when compared to ideal PEC antennas at the same frequency.

B. ANTENNA PERFORMANCE IN TRANSMISSION

In Fig. 8, the radiated fields, given by (44), are shown for different metals as functions of frequency. As expected from the reciprocity principle, the resonances occur at the same frequencies as for the nano-antenna in reception. The analytical and simulation models are with good agreement. In Fig. 9, we illustrate the radiation efficiency e_r given by (47) as function of frequency and for different materials. As can be seen, e_r decreases by increasing the frequency for all four metals. This is because for fixed geometry of nano-antenna, by increasing the frequency, the confinement factor increases, and this limits the radiation efficiency. Among different metals, aluminum has higher efficiency at each frequency, since it has higher absolute permittivity and higher conductivity, resulting into lower confinement factor and lower R_L.

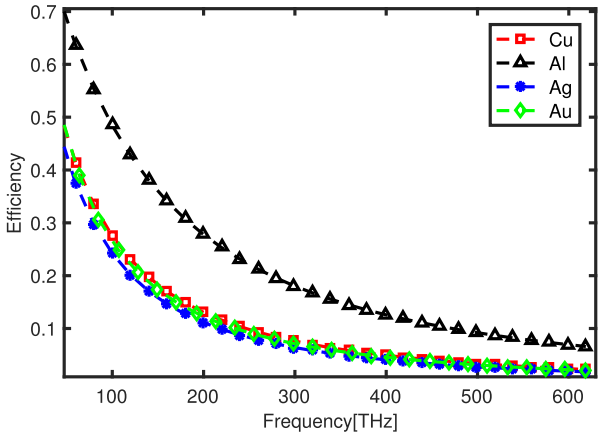

FIGURE 9. Efficiency of different metal.

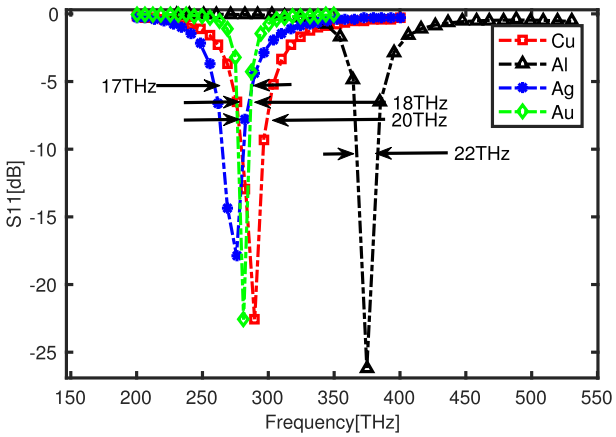

FIGURE 10. S-parameters of 137 nm nano-antenna for different metals.

One last magnitude that is relevant to the nano-antenna performance in transmission and for communication is the 3-dB bandwidth. This can be easily obtained from the S11 parameter or return loss. Fig. 10 shows the antenna behavior for 137 nm nano-antenna and implies that the nano-antenna radiates best at different frequency (as its shown in Fig. 5 with resonance length) with different bandwidth. The figure suggests that bandwidth is roughly highest for aluminum and around 22 THz with better $S11$. The analysis made by COMSOL simulations and allowed us to verify the properties of the antennas with the previous analytical results.

VII. CONCLUSIONS

In this paper, we have developed a unified mathematical framework to analyze the performance of plasmonic nano-antennas in reception and transmission. Starting from the dynamic complex conductivity of the nano-antenna building components, we have formulated the dispersion equation for SPP waves in nano-wires and obtained the SPP wave propagation properties and nano-antenna fundamental resonance length by taking into account also the impact of the nanowire caps. We have then analytically derived an expression for the plasmonic current in the nano-antenna when irradiated by an incident EM wave. In addition, we have derived the radiated fields in transmission as well as the overall radiation efficiency. The analytical models have been then validated by means of FDFD simulations with COMSOL Multi-physics. The agreement between analytical and FDFD data allows us to verify aspects of the model such as far-field as well as near-field properties of the antennas, resonances, reception and emission patterns. We have analytically and numerically shown that the SPP wave confinement factor plays a key role in the nano-antenna efficiency and bandwidth.

ACKNOWLEDGMENT

This paper was presented at the Proceedings of 10th EAI International Conference on Body Area Networks (BODYNETS), 2015 [1].

REFERENCES

[1] M. Nafari and J. M. Jornet, "Metallic plasmonic nano-antenna for wireless optical communication in intra-body nanonetworks," in *Proc. 10th EAI Int. Conf. Body Area Netw. (BODYNETS)*, 2015, pp. 1–7.

[2] I. F. Akyildiz and J. M. Jornet, "Electromagnetic wireless nanosensor networks," *Nano Commun. Netw.*, vol. 1, no. 1, pp. 3–19, Mar. 2010.

[3] H. Guo, P. Johari, J. M. Jornet, and Z. Sun, "Intra-body optical channel modeling for *in vivo* wireless nanosensor networks," *IEEE Trans. Nanobiosci.*, vol. 15, no. 1, pp. 41–52, Jan. 2016.

[4] A. Afsharinejad, A. Davy, B. Jennings, and C. Brennan, "Performance analysis of plant monitoring nanosensor networks at THz frequencies," *IEEE Internet Things J.*, vol. 3, no. 1, pp. 59–69, Jan. 2015.

[5] E. Zarepour, M. Hassan, C. T. Chou, and A. A. Adesina, "Power optimization in nano sensor networks for chemical reactors," in *Proc. ACM 1st Annu. Int. Conf. Nanosc. Comput. Commun.*, 2014, pp. 1–9.

[6] S. Abadal, E. Alarcón, A. Cabellos-Aparicio, M. C. Lemme, and M. Nemirovsky, "Graphene-enabled wireless communication for massive multicore architectures," *IEEE Commun. Mag.*, vol. 51, no. 11, pp. 137–143, Nov. 2013.

[7] P. R. West, S. Ishii, G. V. Naik, N. Emani, V. M. Shalaev, and A. Boltasseva, "Searching for better plasmonic materials," *Laser Photon. Rev.*, vol. 4, no. 6, pp. 795–808, Nov. 2009.

[8] A. Mohammadi, V. Sandoghdar, and M. Agio, "Gold, copper, silver and aluminum nanoantennas to enhance spontaneous emission," *J. Comput. Theor. Nanosci.*, vol. 6, no. 9, pp. 2024–2030, 2009.

[9] A. Boltasseva and H. A. Atwater, "Low-loss plasmonic metamaterials," *Mater. Sci.*, vol. 331, no. 6015, pp. 290–291, Jan. 2011.

[10] T. Stauber, N. M. R. Peres, and A. K. Geim, "Optical conductivity of graphene in the visible region of the spectrum," *Phys. Rev. B, Condens. Matter*, vol. 78, p. 085432, Aug. 2008.

[11] A. Vakil and N. Engheta, "Transformation optics using graphene," *Science*, vol. 332, no. 6035, pp. 1291–1294, 2011.

[12] J. M. Jornet and I. F. Akyildiz, "Graphene-based nano-antennas for electromagnetic nanocommunications in the terahertz band," in *Proc. 4th Eur. Conf. Antennas Propag. (EUCAP)*, Apr. 2010, pp. 1–5.

[13] M. Tamagnone, J. Gomez-Diaz, J. Mosig, and J. Perruisseau-Carrier, "Analysis and design of terahertz antennas based on plasmonic resonant graphene sheets," *J. Appl. Phys.*, vol. 112, no. 11, p. 114915, 2012.

[14] I. Llatser, C. Kremers, A. Cabellos-Aparicio, J. M. Jornet, E. Alarcon, and D. N. Chigrin, "Graphene-based nano-patch antenna for terahertz radiation," *Photon. Nanostruct.-Fundam. Appl.*, vol. 10, no. 4, pp. 353–358, Oct. 2012.

[15] J. M. Jornet and I. F. Akyildiz, "Graphene-based plasmonic nano-antenna for terahertz band communication in nanonetworks," *IEEE J. Sel. Areas Commun.*, vol. 31, no. 12, pp. 685–694, Dec. 2013.

[16] S. Abadal, I. Llatser, A. Mestres, H. Lee, E. Alarcón, and A. Cabellos-Aparicio, "Time-domain analysis of graphene-based miniaturized antennas for ultra-short-range impulse radio communications," *IEEE Trans. Commun.*, vol. 63, no. 4, pp. 1470–1482, Apr. 2015.

[17] J. M. Jornet and A. Cabellos, "On the feeding mechanisms for graphene-based THz plasmonic nano-antennas," in *Proc. 15th IEEE Int. Conf. Nanotechnol. (IEEE NANO)*, Sep. 2015, pp. 168–171.

[18] Q.-H. Park, "Optical antennas and plasmonics," *Contemp. Phys.*, vol. 50, no. 2, pp. 407–423, 2009.
[19] P. Biagioni, J.-S. Huang, and B. Hecht, "Nanoantennas for visible and infrared radiation," *Rep. Progr. Phys.*, vol. 75, no. 2, p. 024402, 2012.
[20] K. J. Vahala, "Optical microcavities," *Nature*, vol. 424, no. 6950, pp. 839–846, Aug. 2003.
[21] L. Feng, Z. J. Wong, R.-M. Ma, Y. Wang, and X. Zhang, "Single-mode laser by parity-time symmetry breaking," *Science*, vol. 346, no. 6212, pp. 972–975, 2014.
[22] Q. Cao and J. Jahns, "Azimuthally polarized surface plasmons as effective terahertz waveguides," *Opt. Exp.*, vol. 13, no. 2, pp. 511–518, 2005.
[23] R. Gordon, "Vectorial method for calculating the Fresnel reflection of surface plasmon polaritons," *Phys. Rev. B, Condens. Matter*, vol. 74, no. 15, p. 153417, 2006.
[24] R. Gordon, "Reflection of cylindrical surface waves," *Opt. Exp.*, vol. 17, no. 21, pp. 18621–18629, 2009.
[25] J. Dorfmuller, R. Vogelgesang, W. Khunsin, C. Rockstuhl, C. Etrich, and K. Kern, "Plasmonic nanowire antennas: Experiment, simulation, and theory," *Nano Lett.*, vol. 10, no. 9, pp. 3596–3603, 2010.
[26] B. Cooper, H. Ehrenreich, and H. Philipp, "Optical properties of noble metals. II.," *Phys. Rev.*, vol. 138, no. 2A, p. A494, 1965.
[27] R. Esteban, A. G. Borisov, P. Nordlander, and J. A. Aizpurua, "Bridging quantum and classical plasmonics with a quantum-corrected model," *Nature Commun.*, vol. 3, p. 825, Apr. 2012.
[28] C. A. Balanis, *Antenna Theory: Analysis and Design*. Hoboken, NJ, USA: Wiley, 2012.
[29] R. L. Olmon and M. B. Raschke, "Antenna—Load interactions at optical frequencies: Impedance matching to quantum systems," *Nanotechnol.*, vol. 23, no. 44, p. 444001, 2012.
[30] P. B. Johnson and R.-W. Christy, "Optical constants of the noble metals," *Phys. Rev. B, Condens. Matter*, vol. 6, no. 12, p. 4370, 1972.
[31] G. Kristensson, S. Rikte, and A. Sihvola, "Mixing formulas in the time domain," *J. Opt. Soc. Amer. A*, vol. 15, no. 5, pp. 1411–1422, 1998.
[32] J.-M. Lourtioz *et al.*, "Photonic crystals and metamaterials," *Comptes Rendus Phys.*, vol. 9, no. 1, pp. 4–15, 2008
[33] M. J. Weber, *Handbook of Optical Materials*, vol. 19. Boca Raton, FL, USA: CRC Press, 2002.
[34] J. Dorfmüller, "Optical wire antennas: Near-field imaging, modeling and emission patterns," Ph.D. dissertation, École Polytechnique Fédérale de Lausanne, 2010.
[35] D. K. Cheng, *Field and Wave Electromagnetics*, vol. 2. New York, NY, USA: Addison-Wesley, 1989.

MONA NAFARI received the B.S. degree in medical engineering (bioelectric) from Islamic Azad University Science and Research Branch, Tehran, Iran, in 2006, and the M.S. degree in electrical engineering (electronics) from Razi University, Iran, in 2010. She is currently pursuing the Ph.D. degree with the Department of Electrical Engineering, University at Buffalo, The State University of New York, Buffalo, NY, USA, under the supervision of Prof. J. M. Jornet. She started her career as a Research Engineer at the Research Center for Science and Technology In Medicine (RCSTIM), Tehran University of Medical Sciences, in 2006. Her current research interests are in optical and terahertz band communication networks and devices and electromagnetic nano-networks.

JOSEP MIQUEL JORNET (S'08–M'13) received the B.S. degree in telecommunication engineering and the M.Sc. degree in information and communication technologies from the Universitat Politècnica de Catalunya, Barcelona, Spain, in 2008, and the Ph.D. degree in electrical and computer engineering from the Georgia Institute of Technology (Georgia Tech), Atlanta, GA, in 2013, with a fellowship from "la Caixa" (2009-2010) and Fundación Caja Madrid (2011-2012). From 2007 to 2008, he was a Visiting Researcher with the Massachusetts Institute of Technology (MIT), Cambridge, under the MIT Sea Grant Program. He is currently an Assistant Professor with the Department of Electrical Engineering, University at Buffalo, The State University of New York. His current research interests are in terahertz-band communication networks, nano-photonic wireless communication, graphene-enabled wireless communications, intra-body wireless nanosensor networks, and the Internet of Nano-Things. He is a member of the ACM. He was a recipient of the Oscar P. Cleaver Award for outstanding graduate students in the School of Electrical and Computer Engineering, Georgia Tech, in 2009. He also received the Broadband Wireless Networking Lab Researcher of the Year Award in 2010. He received the Distinguished TPC Member Award at the IEEE International Conference on Computer Communications in 2016 and 2017. Since 2016, he has been the Editor-in-Chief of the *Nano Communication Networks* Journal (Elsevier).